Supporting Information

Wegmann et al. 10.1073/pnas.1212100110

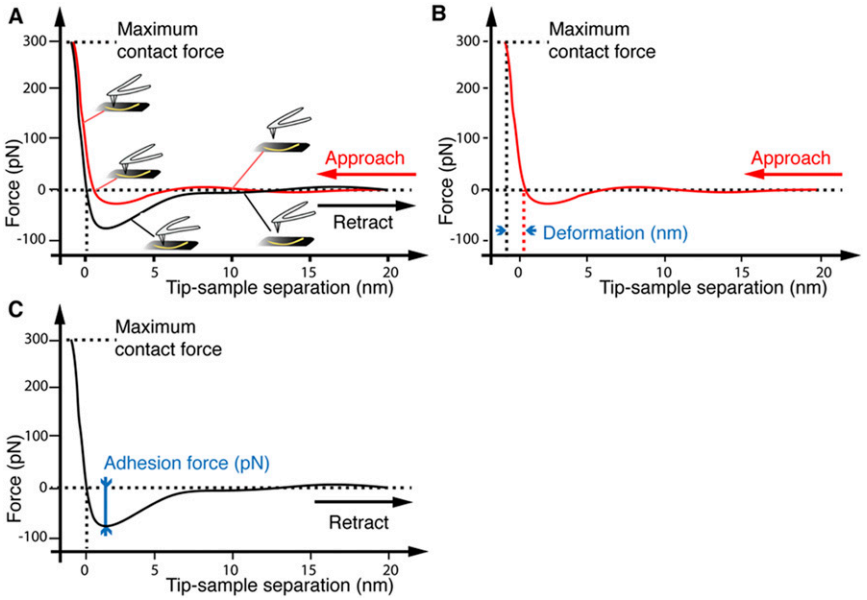

Fig. S1. Force-volume mode atomic force microscopy (FV-AFM) extracts nanomechanical properties from force-distance curves. For every pixel of the topography, FV-AFM records force-distance curves. From these force-distance curves, parameters quantifying the sample properties are derived. (*A*) Approach force-distance curve (red line) records the deflection (force) of the AFM cantilever when approaching the AFM stylus and sample. At a sufficiently small distance, the AFM stylus begins to interact with the sample. Attractive forces pull the AFM stylus toward the sample, and the cantilever deflects downward (negative force). Repulsive forces repelling the AFM stylus and sample deflect the cantilever upward (positive force). The AFM stylus is pressed onto the sample until a preset maximum contact force (imaging force) is reached, which triggers the reversed movement (retraction) of the stylus. During retraction of the AFM cantilever (black line), the cantilever deflection decreases until the contact between the stylus and sample is lost and zero force is detected. (*B*) Sample deformation describes the indentation of the AFM stylus into the (softer) sample at a maximal contact force. (*C*) Adhesion force (negative force) between the AFM stylus and sample is obtained from the retraction force-distance curve (1). The exemplified force-distance curve was recorded on the mica support in buffer solution.

1. Medalsy I, Hensen U, Muller DJ (2011) Imaging and quantifying chemical and physical properties of native proteins at molecular resolution by force-volume AFM. *Angew Chem Int Ed Engl* 50(50):12103–12108.

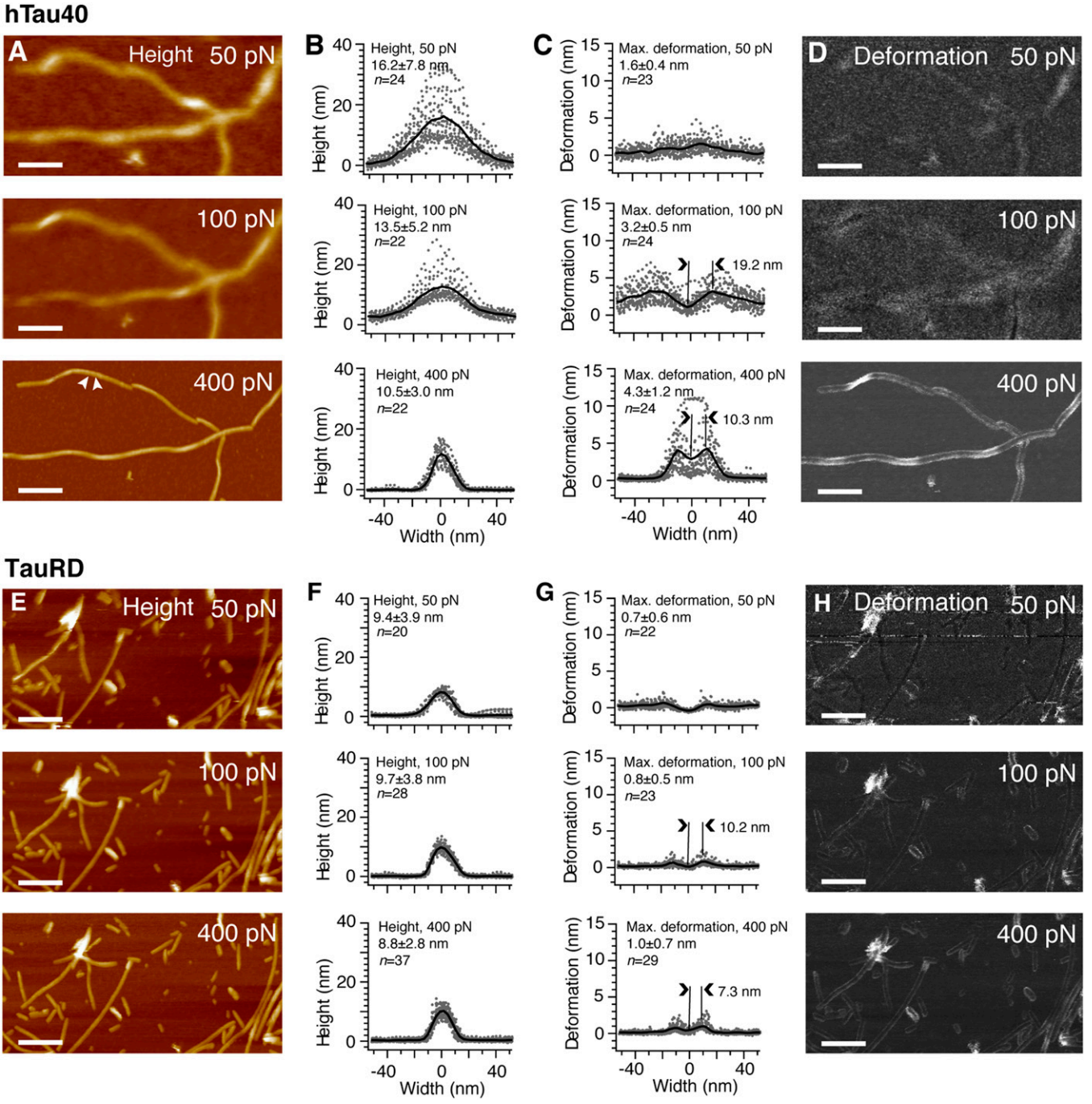

Fig. S2. Force-volume mode atomic force microscopy (FV-AFM) of the longest human Tau protein (hTau40) and Tau repeat domain (TauRD) fibrils at different imaging forces. FV-AFM topographs (*A*) and cross-sectional height profiles (*B*) of hTau40 fibrils imaged at 50 pN, 100 pN, and 400 pN. Deformation profiles (*C*) and maps (*D*) of topographs in *A*. With increasing imaging force, the fibril height decreases (*B*) and deformation increases (*C*). At 50 pN, the deformation [1.6 ± 0.4 nm ($n = 23$)] of the fuzzy coat surrounding the hTau40 fibril occurred over the entire cross-sectional width of the hTau40 fibrils. At 100 pN, maximum (Max.) deformation of 3.2 ± 0.5 nm ($n = 24$) was detected on lanes running parallel to the fibril core (fibril center). (*A*) At imaging forces approaching 400 pN, the soft fuzzy coat was not resolved and the substructure of the core of the hTau40 fibril (1) became visible (white arrowheads). (*D*) Maximum deformation of hTau40 fibrils [4.3 ± 1.2 nm ($n = 24$)] occurred at the edges of the fibril core. This force-dependent appearance of hTau40 fibrils suggests that the extended soft fuzzy coat of hTau40 fibrils is contoured at an imaging force of 50 pN and becomes compressed with increasing imaging force of the AFM stylus. Topographs (*E*) and cross-sectional height profiles (*F*) of TauRD fibrils imaged at 50 pN, 100 pN, and 400 pN and corresponding deformation profiles (*G*) and maps (*H*). Compared with hTau40 fibrils, TauRD fibrils deform much less at imaging forces of 50 pN [0.7 ± 0.6 nm ($n = 22$)], 100 pN [0.8 ± 0.5 nm ($n = 23$)], and 400 pN [1.0 ± 0.7 nm ($n = 29$)]. FV-AFM data were recorded in 10 mM Tris (pH 7.4) and 50 mM KCl. The distance of maximum deformation (black arrowheads in *C* and *G*) to the fibril core center was determined from average profiles (black lines). The number of profiles superimposed and averaged is given by *n*, and values are given as mean ± SD. Full-color scales correspond to a height of 40 nm (*A* and *E*) and a deformation of 15 nm (*D* and *H*). (Scale bars: *A*, *D*, *E*, and *H*; 200 nm.)

1. Wegmann S, et al. (2010) Human Tau isoforms assemble into ribbon-like fibrils that display polymorphic structure and stability. *J Biol Chem* 285(35):27302–27313.

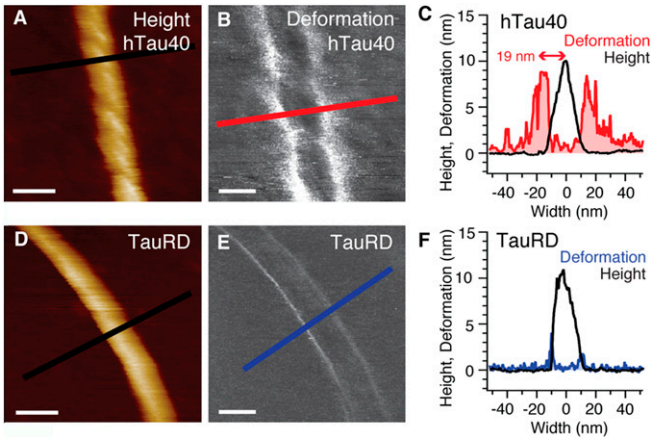

Fig. S3. High-resolution force-volume mode atomic force microscopy (FV-AFM) of Tau repeat domain (TauRD) and the longest human Tau protein (hTau40) fibrils recorded at very low imaging forces of 60 pN. Topography (*A*), a deformation map (*B*), and superimposed cross-section (*C*) of height (black line) and deformation (red line) of the hTau40 fibril are shown. Enhanced deformation is detected on both sides of the rigid (low deformation) hTau40 fibril core. This deformation of the fuzzy coat extends to a distance of 19 nm from the fibril core. Topography (*D*), a deformation map (*E*), and superimposed cross-section (*F*) of height (black line) and deformation (red line) of the TauRD fibril are shown. Minor deformation at the edges of the rigid fibril core indicates the absence of the fuzzy coat in the TauRD fibril. High-resolution FV-AFM images were recorded in PBS, applying an imaging force of 60 pN. (Scale bars: *A*, *B*, *D*, and *E*; 25 nm.)

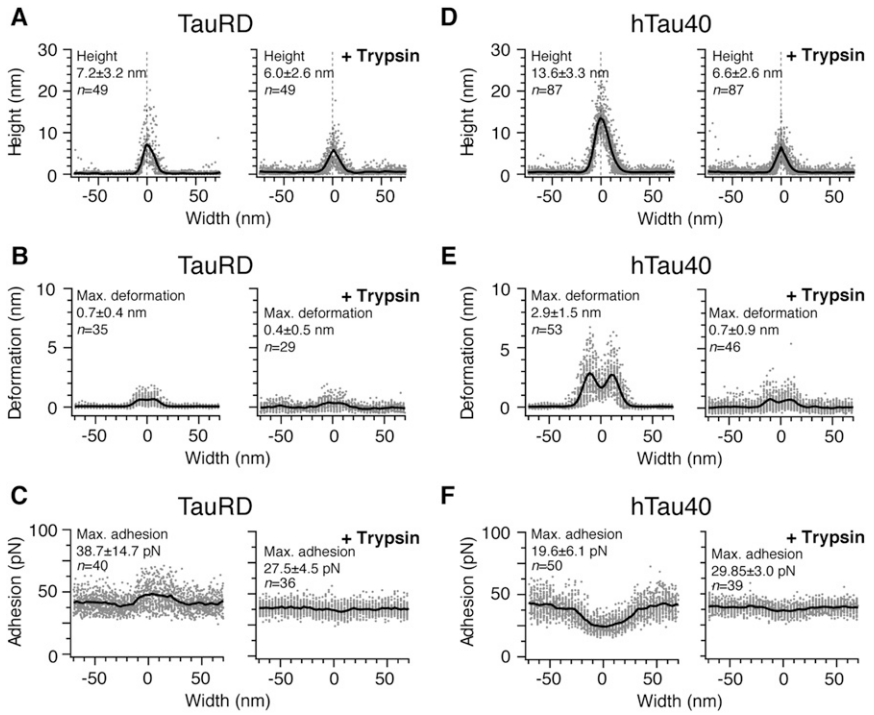

Fig. S4. Height, deformation, and adhesion profiles of Tau repeat domain (TauRD) and the longest human Tau protein (hTau40) fibrils. Scatter plots of height (*A*), deformation (*B*), and adhesion (*C*) cross-section profiles measured from TauRD fibrils before (*Left*) and after (*Right*) trypsin digestion are shown. Profiles were aligned on the topographic fibril center (dashed lines). Scatter plots of height (*D*), deformation (*E*), and adhesion (*F*) cross-section profiles measured from hTau40 fibrils before and after trypsin digestion are shown. Average profiles (mean ± SD) are displayed as black lines, with error bars giving the SD. Mean values of the maximum (Max.) (mean ± SD) are given for each plot. The number of profiles superimposed and averaged is given by *n*, and values are given as mean ± SD. Force-volume mode atomic force microscopy (FV-AFM) images analyzed for this figure were recorded in 10 mM Tris (pH 7.4) and 50 mM KCl, applying imaging forces of 300 pN.

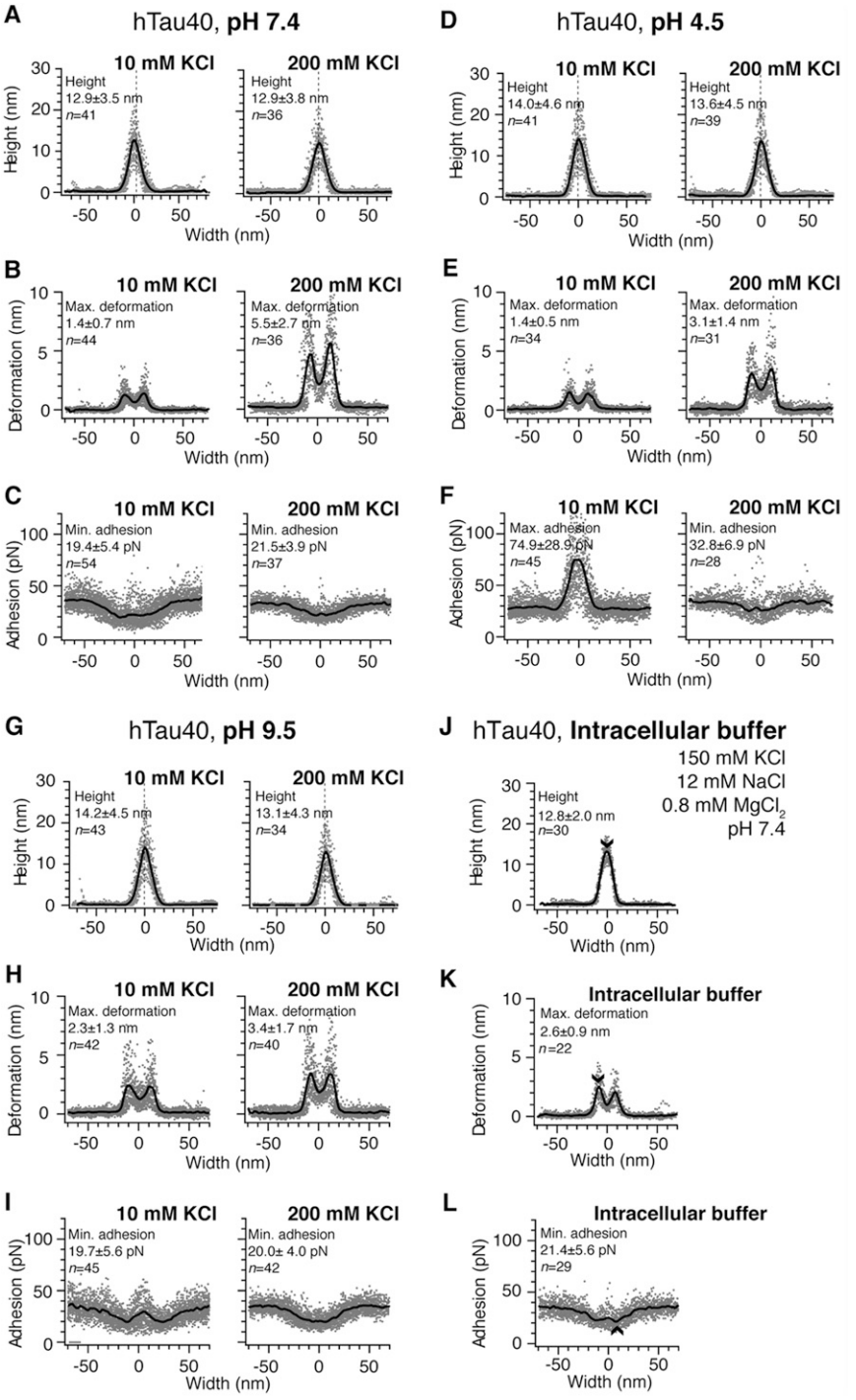

Fig. S5. Cross-section profiles of the longest human Tau protein (hTau40) fibrils reveal salt- and pH-dependent properties of the fuzzy coat. Scatter plots of height (*A*), deformation (*B*), and adhesion (*C*) cross-section profiles measured from hTau40 fibrils at pH 7.4 (10 mM Tris) in 10 mM KCl (*Left*) and 200 mM KCl (*Right*) are shown. Scatter plots of height (*D*), deformation (*E*), and adhesion (*F*) cross-section profiles measured from hTau40 fibrils at pH 4.5 (10 mM sodium acetate) in 10 mM KCl and 200 mM KCl are shown. Scatter plots of height (*G*), deformation (*H*), and adhesion (*I*) cross-section profiles measured from hTau40 fibrils at pH 9.5 (10 mM Tris) in 10 mM KCl and 200 mM KCl are shown. Scatter plots of height (*J*), deformation (*K*), and adhesion (*L*) cross-section profiles of hTau40 fibrils measured in intracellular buffer [150 mM KCl, 12 mM NaCl, 0.8 mM Ca_2Cl (pH 7.4)] are shown. The number of profiles superimposed and averaged is given by *n*. Profiles were aligned on the fibril center (dashed lines). Mean profiles are displayed as black lines. Mean values of the maximum (Max.) (mean ± SD) are given for each condition. Force-volume mode atomic force microscopy (FV-AFM) data analyzed for this figure were recorded applying imaging forces of 300 pN.

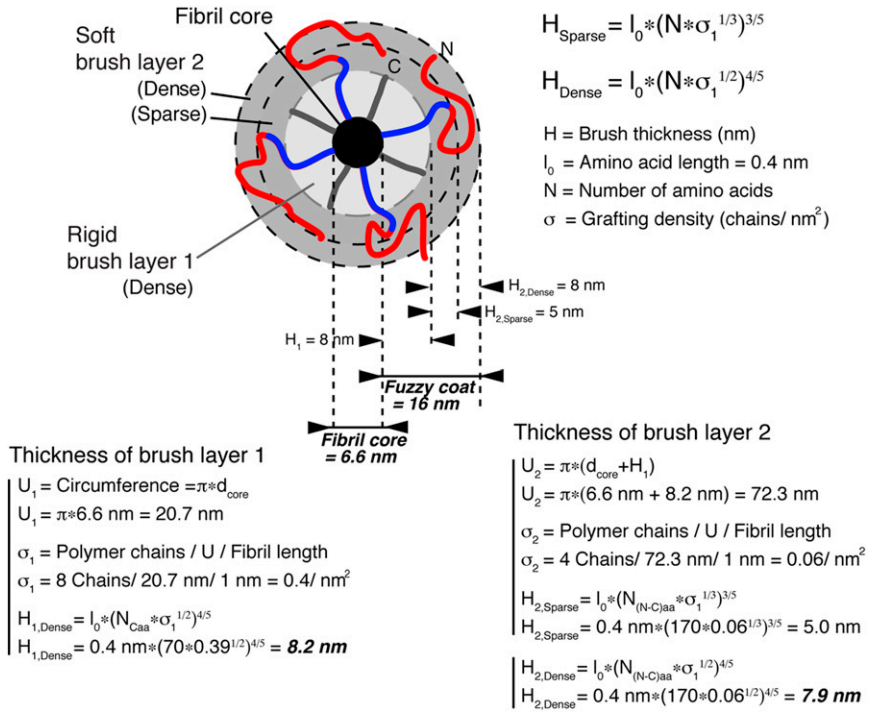

Fig. S6. Dimension of the two-layered polymer brush formed by the fuzzy coat of the longest human Tau protein (hTau40) termini protruding from the Tau fibril core. The thickness, $H = L{\cdot}\sigma^{1/3}$, of planar polymer brushes depends on the grafting density of the polymer chains, σ, and the chain length, L (1). Assuming a polymer chain consisting of N subunits with length, l_0, the chain length is defined as $L = l_0{\cdot}N$ (2). In polypeptides, l_0 describes the average length of amino acids (≈0.4 nm) (3). Applying a spherical brush model (4) the curvature of the grafting surface, which is the fibril core surface, is taken into account. The polymer chain density decreases with radial distance to the fibril core surface. Consequently, the brush thickness decreases to $H_{dense} = l_0(N{\cdot}\sigma^{1/2})^{4/5}$ in dense brushes and to $H_{sparse} = l_0(N{\cdot}\sigma^{1/3})^{3/5}$ in sparse brushes. The fibril core of hTau40 fibrils contains four Tau molecules per nanometer of fibril length (5); has a diameter of ≈6.6 nm and a circumference, U, of ≈20.7 nm (U = pi·diameter); and thus has a grafting density of N and C termini on the fibril core surface of σ ≈ 0.39 per square nanometer. Applying the spherical brush model, we consider a brush containing two layers: (1) a first inner dense brush layer (σ ≈0.39 per square nanometer) in which the C and N termini on the fibril core surface superimpose until the C terminus ends (≈70 aa) and (2) a second outer less dense brush layer (σ = 0.03 per square nanometer) established by the N termini that protrude much further (≈170 aa). The inner "brush layer 1" resembles a dense polymer brush having a thickness of $H_{dense} = l_0(N{\cdot}\sigma^{1/2})^{4/5}$. The outer "brush layer 2" can be modeled as a dense [$H_{dense} = l_0(N{\cdot}\sigma^{1/2})^{4/5}$] or sparse spherical polymer brush with a thickness of $H_{sparse} = l_0(N{\cdot}\sigma^{1/3})^{3/5}$. Considering both possibilities of a two-layered polymer brush, the fuzzy coat exposes a thickness between ≈13 nm and ≈16 nm.

1. deGennes P-G (1980) Conformations of polymers attached to an interface. *Macromolecules* 13(5):1069–1075.
2. Flory PJ (1969) *Statistical Mechanics of Chain Molecules* (Interscience, New York).
3. Pauling L, Corey RB, Branson HR (1951) The structure of proteins; two hydrogen-bonded helical configurations of the polypeptide chain. *Proc Natl Acad Sci USA* 37(4):205–211.
4. Dukes D, et al. (2010) Conformational transitions of spherical polymer brushes: Synthesis, characterization, and theory. *Macromolecules* 43(3):1564–1570.
5. von Bergen M, et al. (2006) The core of tau-paired helical filaments studied by scanning transmission electron microscopy and limited proteolysis. *Biochemistry* 45(20):6446–6457.

Table S1. pH-dependent net charges of hTau40 domains

pH	ND	MD	RD	CD
4	0.6	22.1	24.2	1.8
4.5	**−7.7**	**20.1**	**21.4**	**5.5**
5	−15.1	18.4	18.9	3.5
5.5	−19.1	17.4	17.3	2.3
6	−21.0	16.9	16.0	1.5
6.5	−22.3	16.5	14.5	0.5
7	−23.3	16.2	13.1	−0.4
7.5	**−24.0**	**15.8**	**12.0**	**−1.0**
8	−24.5	15.4	11.0	−1.5
8.5	−24.9	14.8	9.6	−1.9
9	−25.4	13.6	7.7	−2.4
9.5	**−26.4**	**11.2**	**4.2**	**−3.4**
10	−28	6.9	−1.4	5.0

Charges were determined using PROTEIN CALCULATOR v3.3 (The Scripps Research Institute). CD, C-terminal tail domain; MD, middle domain; ND, N-terminal tail domain; RD, repeat domain. Boldface numbers indicate domain charges at pH examined by FV-AFM.